Nanomachines and Other Caps on Mesoporous Silica Nanoparticles for Drug Delivery

Journal:	*Accounts of Chemical Research*
Manuscript ID	ar-2019-001166.R1
Manuscript Type:	Article
Date Submitted by the Author:	n/a
Complete List of Authors:	Chen, Wei; University of California Los Angeles, Chemistry Glackin, Carlotta A.; Beckman Research Institute City of Hope, Stem Cell and Development Horwitz, Marcus; University of California Los Angeles, Medicine Zink, Jeffrey; University of California Los Angeles, Chemistry and Biochemistry

Nanomachines and Other Caps on Mesoporous Silica Nanoparticles for Drug Delivery

Wei Chen,[†,§] Carlotta A. Glackin,[‡] Marcus A. Horwitz,[#] Jeffrey I. Zink[†,§,]*

† Department of Chemistry & Biochemistry, University of California Los Angeles, Los Angeles, California 90095, United States

§ California NanoSystems Institute, University of California Los Angeles, Los Angeles, California 90095, United States

‡ Department of Stem Cell and Developmental Biology, City of Hope–Beckman Research Institute, Duarte, California 91010, United States

Division of Infectious Diseases, Department of Medicine, University of California Los Angeles, California 90095, United States

CONSPECTUS

Mesoporous silica nanoparticles (MSNs) are delivery vehicles that can carry cargo molecules and release them on command. The particles used in the applications reported in this Account are around 100 nm in diameter (about the size of a virus) and contain 2.5 nm tubular pores with a total volume of about 1 cm^3/g. For the biomedical applications discussed here, the cargo is trapped in the pores until the particles are stimulated to release it. The challenges are to get the particles to the site of a disease and then to deliver the cargo on command. We describe methods to do both and we illustrate the applicability of the particles to cure cancer and intracellular infectious disease.

Our first steps were to design multifunctional nanoparticles with properties that allow them to carry and deliver hydrophobic drugs. Many important pharmaceuticals are hydrophobic and cannot reach the diseased sites by themselves. We describe how we modified MSNs to make the dispersable, imagable and targetable and discuss *in vitro* studies. We then present examples of surface modifications that allow them to deliver large molecules such as siRNA. *In vivo* studies of siRNA delivery to treat triple negative breast and ovarian cancers are presented.

The next steps are to attach nanomachines and other types of caps that trap drug molecules but release them when stimulated. We describe nanomachines that respond autonomously (with human intervention) to stimuli specific to disease sites. A versatile type of machine is a nanovalve that is closed at neutral (blood) pH but opens upon acidification that occurs in endolysosomes of cancer cells. Another type of machine, a snap-top cap, is stimulated by reducing agents such as glutathione in the cytosol of cells. Both of these platforms were studied *in vitro* to deliver antibiotics to infected macrophages and *in vivo* and cure and kill the intracellular bacteria *M. tuberculosis* and *F. tularensis*. The latter is a tier 1 select agent of bioterrorism.

Finally, we describe nanomachines for drug delivery that are controlled by externally administered light and magnetic fields. A futuristic dream for nanotherapy is the ability to control a nano-object everywhere in the body. Magnetic fields penetrate completely and have spatial selectivity governed by the size of the field-producing coil. We describe how to control nanovalves with alternating magnetic fields (AMF) and superparamagnetic cores inside the MSNs. The AMF heats the cores and temperature sensitive caps release the cargo. *In vitro* studies demonstrate dose control of the therapeutic to cause apoptosis without overheating the cells. Nanocarriers have great promise for therapeutic applications, and MSNs that can carry

drugs to the site of a disease to produce a high local concentration without premature release and off-target damage may have the capability of realizing this goal.

1. INTRODUCTION AND BACKGROUND

The development of mesoporous silica nanoparticles in our research group for biomedical applications began with a completely unrelated line of research: investigation of transparent matrices for room temperature matrix isolation spectroscopy. The popularity of sol-gel synthesis of inorganic metal oxides was on the rise, and silica seemed to be a promising matrix candidate. The precursors, tetraalkoxy silanes, alcohol and water were readily available, and the formation of monolithic silica glass by hydrolysis and condensation occurred at room temperature in the air.[1]

Molecules of spectroscopic interest to us dissolved in the initial sol and the glass formed around them and trapped them. Under acidic conditions and slow drying (to prevent cracking) in a cuvette, beautiful transparent rectangular prismatic pieces of glass were formed. Because of the mild synthesis conditions, even delicate biomolecules such as enzymes and other proteins could be trapped and retain their functions.[2–5]

The next important step was stimulated by reports that surfactant molecules coupled with the sol-gel synthesis could template well-ordered pores.[6] Liquid crystalline phases such as rods or sheets could template tubular and lamellar structures. When the surfactant was removed by extraction or heating the former phase produced 2-dimensional hexagonal pores. (These structures were actually reported in the patent literature 20 years earlier but not appreciated at that time.)[7] The original morphologies were macro-sized translucent pieces, but we wanted uniform transparent pieces so we explored and develop methods of synthesizing thin films.[8–11]

We prepared and studied photophysical properties of molecules trapped in films on the order of 100 nm thick.

The final step was the discovery that under basic conditions, nanoparticles of the templated silica could be prepared.[12] Formation of monodisperse particles was very sensitive to not only the concentrations of reactants but also to temperature and stirring speed in a flask. A cascade of synthetic papers followed and now it is standard to produce particles under 100 nm in diameter with highly ordered porosity.[13–18] These particles are generally called "mesoporous silica nanoparticles" or MSNs (Figure 1AB). The MSNs that will be described in this account typically have a diameter of about 100 nm with 2.5 nm tubular pores, a surface area of about 1000 m^2/g and a volume of about 1 cm^3/g.[19,20]

As the synthetic challenges were being overcome, the question became what to do with the particles? In our work, we adapted multiple techniques that we had developed for attaching molecules to films to derivatizing the particles' surfaces (both the outer particle surface and the huge internal pore surfaces).[19] Attachment of fluorescent dye molecules enabled the particles to be tracked by optical spectroscopy (even though the particles themselves were only imageable by transmission electron microscopy). After derivatization and surfactant extraction, the empty pores invited being filled with other molecules, and drug molecules brought the MSNs into the biomedical world.

2. *IN VITRO* HYDROPHOBIC DRUG DELIVERY

Our first foray into *in vitro* applications of our particles involved hydrophobic anticancer drugs as the cargo molecules in the pores.[21] A challenge in cancer therapy is to deliver hydrophobic drugs to the sites of the disease. Many important anticancer drugs are poorly soluble and some sort of delivery system is needed. (The most important such systems currently

in use are liposomes and albumins.) We wanted to see if MSNs could be suitable. A problem immediately arose: MSNs as synthesized aggregated extensively in water and biorelevant fluids. To achieve dispersity, we attached and tested many different types of molecules and settled on phosphonate for our initial studies and fluorescein as our fluorescent label. Anionic phosphonate groups were attached by using trihydroxylsilylpropylphosphonate (THMP). This choice was unconventional because the current lore stated that positively charged particles would be better taken up by cells. It turned out to be a great choice because the particles had good circulation times in mice, were endocytosed readily by cancer cells, and accumulated in xenograft tumors as will be discussed later.

Our first demonstration of hydrophobic drug delivery used camptothecin (CPT), a representative anticancer drug that is also fluorescent. Derivatives of CPT are promising and effective drugs against a wide variety of carcinomas, but have much lower cytotoxicity than CPT. (FDA approved Irinotecan has a potency of 10% of that of CPT.) CPT was loaded into the pores by soaking MSNs in a DMSO solution of the drug overnight. The loaded nanoparticles were sonicated and washed with PBS solution to remove any weakly adsorbed drugs from the surfaces. A dispersion of the CPT-loaded MSNs was added to PANC-1 cells to determine if the nanoparticles transported the CPT into the cells and fluorescence microscopy was used to monitor the uptake. The delivery inhibited growth and caused apoptotic cell death.

We have also utilized mesoporous organosilica nanoparticles (MONs) and a chaperone-assisted strategy to facilitate both the loading and the release of hydrophobic drugs from nanoparticles. MONs have bridged organoalkoxysilanes in their frameworks that enable a very high loading of hydrophobic drugs in their pores. We used biodegradable oxamide-phenylene based MONs to achieve 84 wt% of hydrophobic CPT and CPT delivery in lung cancer cells.[22]

For pure MSNs, we recently developed a chaperone-assisted strategy to achieve both substantial loading and release amounts of the water-insoluble drug clofazimine (CFZ).[23] The interaction between the chaperone acetophenone (AP) molecules and CFZ provides the driving force for AP to carry large concentrations of CFZ into the pores, and thus significantly enhances the release of CFZ in buffer solution. *In vitro* studies show that the optimized CFZ-loaded MSNs effectively kill *Mycobacterium tuberculosis* in macrophages. This chaperone-assisted delivery strategy can be applied to the loading and delivery of other hydrophobic drugs with their suitable chaperone molecules.

3. MULTIFUNCTIONAL MSNS

The MSNs used in the hydrophobic CPT delivery study had two different molecules attached to their surfaces: phosphonate for dispersibility and fluorescein for optical imaging. We wanted to push the limits and to demonstrate that more functionality and versatility could be achieved (Figure 1A). To that end, we synthesized a different type of MSN containing a superparamagnetic iron oxide core for magnetic manipulation and MRI imaging (Figure 1C).[19] The pores were available for filling with cargo. On the outer surface we attached a biomolecule, folate, that we wanted to test for active targeting of cancer cells. The resulting paper had a large impact because it brought attention to the versatility of MSNs as a platform for multiple actions including imaging and drug delivery.

An important aspect of our explorations of multifunctional MSNs was our investigation of active targeting agents. In order to be effective therapeutic agents, MSNs need to be carried "passively" by the blood to the site of the tumor. In addition, "active" targeting of specific receptors on tumor cells could be achieved by attaching appropriate molecules to the MSNs. Our initial studies involved folate and we found that uptake of the particles by cells having folate

receptors was almost always enhanced *in vitro* but that *in vivo* tumor shrinkage was often but not always enhanced. Similar results were obtained with MSNs containing attached ferritin and an RGD peptide.[24] Excellent results with hyaluronic acid are discussed in the following section. It is clear that active targeting can occur but each type of targeting agent must be evaluated on a case by case basis.

We further extended the functionality of MSNs by coating the outside surface with polymers. The two most important polymers (evidenced by the *in vitro* and *in vivo* studies described in detail below) were PEG and low molecular weight PEI (Figure 1D). In some cases, we chemically bonded the PEI to the particles and in others we used electrostatic attraction of the cationic PEI to the anionic phosphonate-coated surface. We showed that low molecular weight PEI (1.2 kD) has negligible toxicity compared to that of the high molecular weight polymer.[25] Its importance lies in its abilities to carry, protect and deliver siRNA (next section) as well as to facilitate endosomal escape through the proton sponge effect for the nucleotide delivery. The PEG coatings were used to improve dispersibility and also for their ability to increase circulation time in mice (stealth particles).[26]

4. NANOPARTICLE DELIVERY OF SMALL INTERFERING RNAS – FROM BASIC SCIENCE TO CLINICAL APPLICATIONS

Recently efforts have begun to use siRNA as a therapeutic agent.[27] Preclinical and clinical trials have demonstrated that siRNA can be delivered to cells *in vivo* and retain its function, knocking down target genes in both prostate cancer and melanoma.[27] A drawback to RNAi-based therapy is that RNA tends to be susceptible to nuclease degradation, and is thus unstable in the body. Our polymer-coated MSNs proved to be very effective in protecting siRNA and carrying it to tumors in mice.

RNA interference (RNAi) using double-stranded RNA was first demonstrated in *C. elegans*.[27,28] In mammals, 21-nucleotide long RNA fragments called small interfering RNAs (siRNAs) are the effectors of RNAi.[29] These fragments bind to a target mRNA, and then form the RNA induced silencing complex (RISC).[30] RISC also contains Argonaute proteins, specifically Ago2, that cleave the mRNA, thus preventing protein translation.[31]

Our earliest successful demonstration of RNA delivery using MSNs involved delivery of siRNA to drug-resistant KB-V1 cells to silence the expression of efflux transporter P-glycoprotein (PPgp). We used low molecular weight cationic PEI coating (described in section 3) in which the anionic siRNA was entrained and protected. Dox was loaded in the pores.[32] The dual delivery demonstrated that MSN delivery effectively knocked down gene expression of a drug exporter and increased intracellular DOX levels to improve cytotoxic killing.[32]

We have recently shown *in vivo* efficacy of MSN-delivered siRNA in a mouse model of melanoma. Mice treated with siRNA against *TWIST* had smaller, less vascularized tumors, likely the result of inhibition of CCL2-driven angiogenesis within the growing tumors.[33] We obtained similar data in ovarian cancer, where mice treated with siTWIST-MSN plus chemotherapy had 75% less tumor burden than control mice treated with chemotherapy only.[34]

In a second series of studies, we combined active targeting of Cancer Stem Cells (CSC) with siRNA delivery (Figure 2).[35] Cluster of differentiation 44 (CD44) is a ubiquitously present glycoprotein on the surface of mammalian cells. Since the discovery that the receptor is over-expressed in a variety of solid tumors, such as pancreatic, breast and lung cancer, many studies have focused on methods for targeting CD44 in an attempt to improve drug delivery and discrimination between healthy and malignant tissue, while reducing residual toxicity and off-target accumulation. Hyaluronic acid (HA), the primary CD44 binding molecule, has proved a

significant ally in developing nanocarriers that demonstrate preferential tumor accumulation and increased cell uptake.

We studied HA-coated MSNs as a therapeutic approach to deliver oligonucleotides to tumors that overexpress CD44+ (Figure 3).[35] We delivered TWIST siRNA to breast and ovarian cancer xenografts and reduced tumor burden.[33–35] Our particles inhibited EMT signaling, reduced tumor burden and exhibited synergistic efficacy in combination with cisplatin.[35] These results demonstrated a useful therapeutic strategy for chemoresistant ovarian cancer. Successful application of these types of approaches could pave the way for future RNA-based therapies against other targets of interest currently thought to be "undruggable".

5. NANOMACHINES

Our next major goal was to design a system that could carry a therapeutic through the blood stream to the site of a disease with no leakage, release a high local concentration of the drug, release it only on an autonomous or external command, and kill the cancer cells or an infectious agents. The release itself required a pore cap that could be closed to trap cargo molecules and open in response to a desired stimulus and release the cargo.[13,15,20,36] We named our original system a "nanovalve" which consisted of a stalk and a large cyclic molecule that blocked the pore in the closed position and slid along the stalk away from the pore opening to release the pore's contents. The large amplitude motion of this nanomachine, like that of any machine, needs a power supply. What kinds of motions and what kinds of stimuli could we use that would be compatible with a machine deep in the body of an animal? Answering these questions and making suitable machines required both imagination and hard work.

We categorize nanomachines according to the source of the stimulus required to operate them (Figure 1E).[14] When the stimulus is a direct result of human intervention, we call it

"external". The most important external sources are light, magnetism and ultrasound. Each of these sources can produce large amplitude motion in molecules by multiple mechanisms. For example, light energy can cause photochemical reactions, produce heat that causes a chemical reaction, or be absorbed by "transducer" molecules that change the pH (photoacids) or cause electron transfer (photooxidants or reductants). Heat production is the primary usable effect of alternating magnetic fields and ultrasound.

The second category of operation we call "internal" or "autonomous". The stimulus for operation originates from the change in the particles' surroundings. For example, when the machine goes from the blood stream to a cell's endolysosome as a result of endocytosis, the pH changes from 7.4 to less than 6 and a pH sensitive valve opens. When it enters the cytosol, the presence of antioxidants such as glutathione cause a redox active valve to open. No external intervention is required. Autonomous nanomachines such as these are the most widely studied *in vitro* and *in vivo*.

The most actively studied pH valve is based on the design principle of a cyclic cap that has a large binding constant to a stalk that is hydrophobic at the pH of blood but becomes protonated and hydrophilic in the acidic environment of an endolysosome. A widely used example is shown in Figure 4.[37] The cyclic molecule is β-cyclodextrin (βCD), a cyclic sugar with a hydrophobic interior. The stalk is a specific benzimidazole with a pKa of about 7. Above pH 7, the hydrophobic-hydrophobic non-covalent interaction holds the pseudorotaxane together but at lower pH it dissociates. When the stalk is attached at a pore opening on MSNs, the βCD traps cargo molecules in the pore but releases them upon acidification. *In vivo* applications of this autonomous pH nanovalve are discussed in the following section.

The most-used redox activated system that we named a "snap-top" is based on the design principle that a redox-sensitive chemical bond can be broken in the presence of reducing agents in the cytosol of a cell.[38] This simple design utilizes a disulfide stalk containing a bulky cap on its end (Figure 5). When attached at an MSNs pore surface the cap traps the cargo, but when the particle escapes the lysosome the reducing agents such as glutathione cause the disulfide to dissociate into two thiols, releasing the bulky group and the trapped drug molecules. *In vivo* studies using this redox snap-top are described in the following section.

Many other autonomous nanomachines and capping agents have been studied and several thorough reviews have been published recently.[13,15,20] One additional example from our group is the original enzyme-activated snap-top in which a βCD slides on a stalk but is blocked from leaving by a bulky stopper held in place by a functional group (an ester) that is a substrate for an enzyme (porcine liver esterase).[39] When the particle encounters the enzyme the bulky group is "snapped off" and the cargo is released. This type of snap-top is a prototype for a nanocarrier that could respond only to a specific enzyme overexpressed by a particular cancer cell.

6. NANOPARTICLES AGAINST INFECTIOUS DISEASES CAUSED BY INTRACELLULAR PATHOGENS

We used both of the nanomachines in Figures 4 and 5 to kill pathogenic bacteria in phagocytes *in vitro* and in *vivo*. Mononuclear phagocytes, primarily monocytes and tissue macrophages, are known as professional phagocytes because of their reputation for avidly ingesting particles of many kinds. Such particles include numerous pathogens that are readily killed by macrophage antimicrobial armaments. However, one class of pathogens, known as intracellular parasites, intentionally induce their uptake by macrophages with the aim of hijacking host cell machinery towards their own end – survival and intracellular replication.

Intracellular pathogens include the agents of tuberculosis and what are referred to by the US government as Tier 1 Select Agents because of especially high concern that they may be intentionally employed in a bioterrorist attack. Such pathogens include *Francisella tularensis*, the agent of tularemia.

For treatment of many diseases, mononuclear phagocytes – especially those in the liver, spleen and lung – pose an obstacle to MSN delivery of nanotherapeutics, since they readily ingest intravenously administered nanoparticles intended for delivery elsewhere, *e.g.* to cancer cells. MSNs designed for cancer therapy need to be specially designed to evade macrophages, but for treatment of diseases caused by intracellular pathogens, the avidity with which macrophages ingest MSNs provides a tremendous advantage – no specific targeting ligands are necessary to deliver copious amounts of antibiotic-loaded particles to macrophages harboring intracellular pathogens. Nanotherapeutic delivery of antibiotics maximizes antibiotic delivery to infected host macrophages while minimizing systemic toxicity.

Our nanotherapeutics have been designed primarily to treat two diseases caused by intracellular pathogens – tuberculosis, caused by *Mycobacterium tuberculosis* (Mtb),[23,40,41] and tularemia, caused by *Francisella tularensis* (Ft).[42,43] Both diseases pose major challenges to treatment with conventionally delivered antibiotics. TB caused by drug-sensitive organisms requires 6-9 months treatment and drug-resistant Mtb, which is even more difficult to treat requires multidrug therapy for up to 2 years. Hence, more efficient delivery of antibiotics to host macrophages via nanotherapeutics has the potential to shorten the treatment course, improve adherence, impede the emergence of drug resistance, and reduce systemic drug toxicity.

Tularemia, a bacterial zoonosis, can manifest as one of several syndromes depending upon the mode of Ft transmission. Pneumonic tularemia, the most dangerous form and the one of

greatest concern from a bioterrorism perspective, is contracted via inhalation. With current therapy, tularemia can still be fatal, resolve slowly, or relapse. Hence functionalized nanotherapeutics targeting infected macrophages have the potential for more rapid cure, reduced time in intensive care, and less frequent relapse.

We designed and evaluated PEI-coated MSNs (~100 nm) loaded with the antibiotic drug Rifampin for treatment of TB.[41] These MSNs were all avidly ingested by Mtb-infected human macrophages (Figure 6A). By fluorescence microscopy, the MSNs co-localized with CD63, indicating uptake into endolysosomes.[41] In *In vitro* studies in which these MSNs were added to human macrophages infected with the highly virulent Mtb Erdman strain, the MSNs readily killed Mtb, and they did so significantly more efficiently than an equivalent amount of free drug (Figure 7A).

We developed MSNs with pH- and redox potential- sensitive nanovalves for delivery of the antibiotic moxifloxacin (MXF).[42,43] Both types of MSNs were avidly ingested by Ft-infected macrophages (Figure 6B) and rapidly killed intramacrophage Ft in a dose-dependent fashion. These MSNs were evaluated for efficacy in a murine model of lethal pneumonic tularemia in which mice were infected intranasally with a lethal dose of Ft LVS ($6xLD_{50}$). The mice were treated with free MXF or MXF-loaded MSNs intavenously every other day for three doses; euthanized one day later; and Ft CFU assayed in lung, liver, and spleen. In untreated mice, bacteria multiplied to high levels (~7.5 logs in the lung) and the mice lost 12-24% of their total body weight. In contrast, mice treated with MXF-loaded MSNs maintained their body weight and CFU in the lungs decreased by 1-2 logs (Figure 7B).[43] The MXF-loaded MSNs were significantly more effective than an equivalent amount of free drug in reducing CFU in all organs; in the lung, they were more effective than ~3 fold greater dose of free MXF.

7. EXTERNALLY OPERATED NANOMACHINES AND CAPS

A futuristic dream for nanotherapy is the ability to control a nano-object everywhere in the body. Although total control including mobility is far from reality, it is possible to stimulate nanocarriers anywhere and to release therapeutic molecules with spatial and temporal accuracy. The major methods of external control are light, ultrasound and magnetism. For diseases on or near the skin, photothermal therapy is useful, but for tumors deep in the body, magnetism penetrates the best. Externally operated drug release is a step beyond autonomous release because it can be turned on and off at will and does not have to rely on specific chemical changes or the presence of specific molecules in order to operate. It is also more complex than autonomously stimulated release because the external control also requires external instrumentation and an operator. These issues contribute to the sparsity of *in vivo* studies reported to date.

Progress in synthesizing and making functioning nanomachines and caps that can be remotely activated has been rapid.[13,14,20,36] The most prevalent and highly developed systems are light activated. We were interested in using light to power nanomachines, including by direct photochemical bond breaking or photoisomerization and by indirect phototransducers to activate pH and redox valves. Direct photocleavage is a convenient way to remove caps from pores. Molecules in their excited state can transfer protons (photoacids)[44] or electrons (photo-redox)[45] and can be used to activate machines originally designed to be activated by chemical acidification or redox. Excited state energy transfer from molecules with high two photon cross sections can trigger the above reactions using two near infrared photons.

We used our impeller for our first *in vitro* studies.[46] Photo-induced trans-cis isomerization of azobenzene derivatives bonded to the insides of MSN pore walls trap cargo

molecules in the dark but allow them to escape when they wag back and forth.[47,48] We delivered an anticancer drug into pancreatic cancer cells and observed no killing in the dark but efficient apoptosis when the impellers were excited.[46]

Other photo-responsive gatekeepers include azobenzene and cyclodextrin supramolecular complex,[49,50] photolabile coumarin-based nanovales,[51] cucurbit[6]uril (CB[6]) and stalk supramolecular complexes,[52] photoacid molecules and pH-sensitive nanovalves,[44] and photo-transduced molecules and redox environment-sensitive nanovalves.[53] We later demonstrated two photon near IR excitation of a transducer molecule that transferred energy to the azobenzene molecules and released cargo.[54] Interesting progress continues to be made in the two-photon field for potential biomedical applications.

In our current research for biological applications, we are focusing on magnetism as the stimulus, specifically alternating magnetic fields (AMF). Nanoparticles containing superparamagnetic components are heated by the AMF and thermo-stimulated machines or caps can be activated by the heat to release cargo. Magnetic heating is currently being used to kill cells or destroy tumors by hypothermia,[55–57] but it can also create tumor metastasis. We are focusing on drug delivery by taking advantage of the localized particle heating without bulk heating.

To understand what degree of local heating can be attained, we designed nanothermometers in the MSNs containing the superparamagnetic heaters and measured internal temperature changes of over 20 °C above that of the surrounding aqueous medium, more than enough to activate thermosensitive caps without causing hyperthermia.[58–60]

Our first *in vitro* study used core@shell nanoparticles to carry and deliver drugs actuated by AMF and used a supramolecular valve comprised of a bulky cucurbit[6]tril (CB[6]) ring and an

alkylammonium thread attached on the surface of MSNs that acts as a thermo-sensitive gatekeeper (Figure 8).[61] When the temperature increases, the binding constant between the CB[6] ring and the alkylammonium thread decreases leading to the detachment of CB[6] from the thread followed by drug release. The release of drugs was not triggered by bulk heating from the solutions but by localized heating generated from the interior magnetic cores. We showed that doxorubicin released intracellularly by AMF stimulation effectively kills MDA-MB-231 breast cancer cells.

Very recently, we demonstrated spatial, temporal, and dose control of drug delivery using superparamagnetic $MnFe_2O_4$@$CoFe_2O_4$ nanoparticles with high specific loss power (1510.8 W/g) and high saturation magnetization (105 emu/g) (Figure 9).[62] Thermo-sensitive gatekeepers that contain an aliphatic azo moiety release a bulky cap and regulate the release of drugs. The dose of the drug release was controlled by the AMF exposure time and triggered by the localized high temperature from the interior magnetic core and not by bulk heating. Multiple sequential exposure of AMF causes drug release in a step-wise manner. *In vitro* studies show that the drug delivery platform is biocompatible, that drug-loaded nanocarriers do not kill the cells without the AMF stimulation, and that cell death was correlated with the AMF exposure time (Figure 10). Thermo-responsive drug delivery stimulated by an AMF offers the potential of becoming an innovative chemotherapy that noninvasively, remotely, and precisely controls the dosage of drugs, avoiding the risk generated when overheating the bulk solution.

8. FUTURE PERSPECTIVES

Mesoporous silica is a versatile platform for drug delivery applications. The nanoparticles are nontoxic, carry large payloads of therapeutic drugs, and can be capped to prevent premature drug release until the nanoparticles reach their target where they can then be stimulated to release a

high local concentration of the therapeutic. The particles can carry other important therapeutic molecules such as siRNA, protect them from enzymes and degradation, and release them intracellularly. Their potential for curing cancer occupies most current research attention, but they can be used to treat other diseases including infectious diseases.

The route of administration is important. We emphasized intravenous administration, but for treatment of intracellular pathogens, we found that intramuscular injection was extremely beneficial because of superior pharmacokinetics.[63] Preliminary studies show inhalation administration to be extremely promising for treatment of lung infections.

The multifunctionality of nanotherapeutics including MSNs promises to revolutionize drug delivery. It allows for active targeting of drug-loaded particles (– our best *in vivo* example of a successful agent is hyaluronic acid – other targeting agents (*e.g.* folic acid, and RGD peptide) toward their specific cancer cells were also demonstrated). The drug-loaded particles can additionally contain molecules for image guided therapy, such as paramagnetic metals or superparamagnetic cores for imaging by MRI, fluorescent dyes (especially in near-IR for optical imaging), and atoms for PET imaging. The multifunctionality of nanotherapeutics also allows for theranostics – the combining of therapeutic and diagnostic agents into a single nanoparticle. Finally, the multifunctionality of nanotherapeutics allows for the delivery of combination drug therapy at optimal drug dose ratios, thereby enhancing drug synergy and safety.

It would be extremely beneficial if MSNs could move forward toward clinics. Before then, many prerequisites need to be fulfilled, such as industrial-scale production of MSNs under Good Manufacturing Practice (GMP) to guarantee that the properties of the MSNs are reproducible from batch to batch, detailed investigations of the potential toxicity, bio-distribution, and clearance from the animal body, and whether drug-loaded MSNs have higher treatment efficacy

and fewer side effects than those of the free drugs alone. It is a long and complicated road to clinical trials and eventual use in the clinic, but the attractive properties make MSNs worthy of the attention that they are being given.

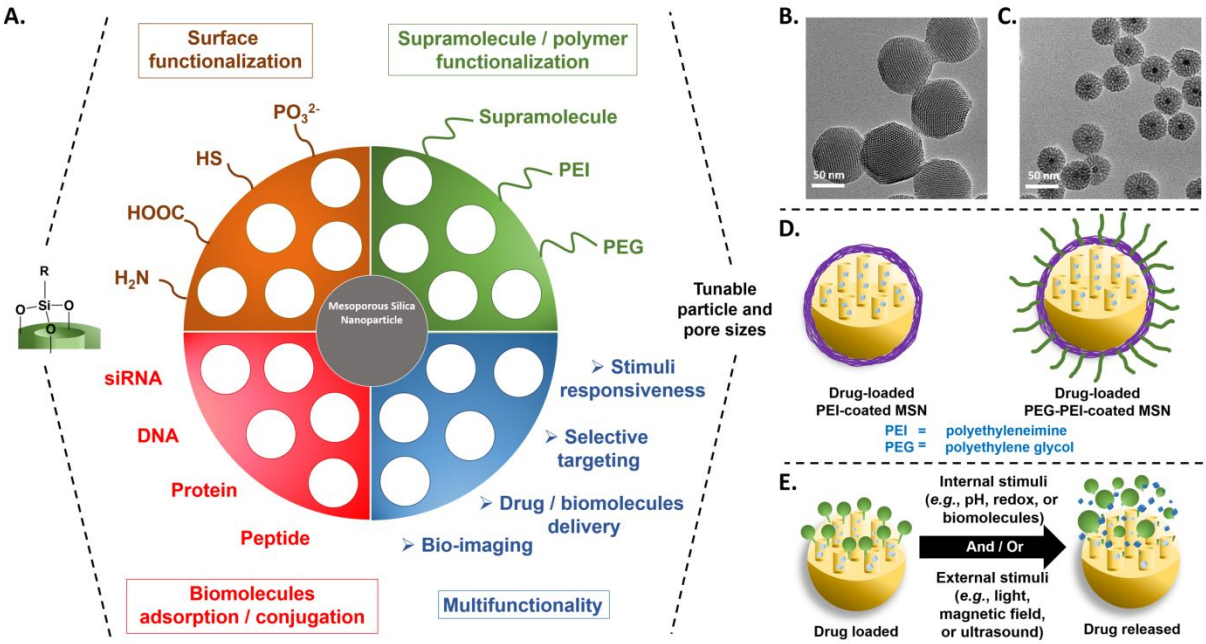

FIGURE 1. Collage of MSNs described in this Account. (A) Overview of functionalities of MSNs. Portrait of (B) MSNs and (C) magnetic core@shell nanoparticles. (D) Polymer coating. (E) Stimuli-responsive drug release particles.

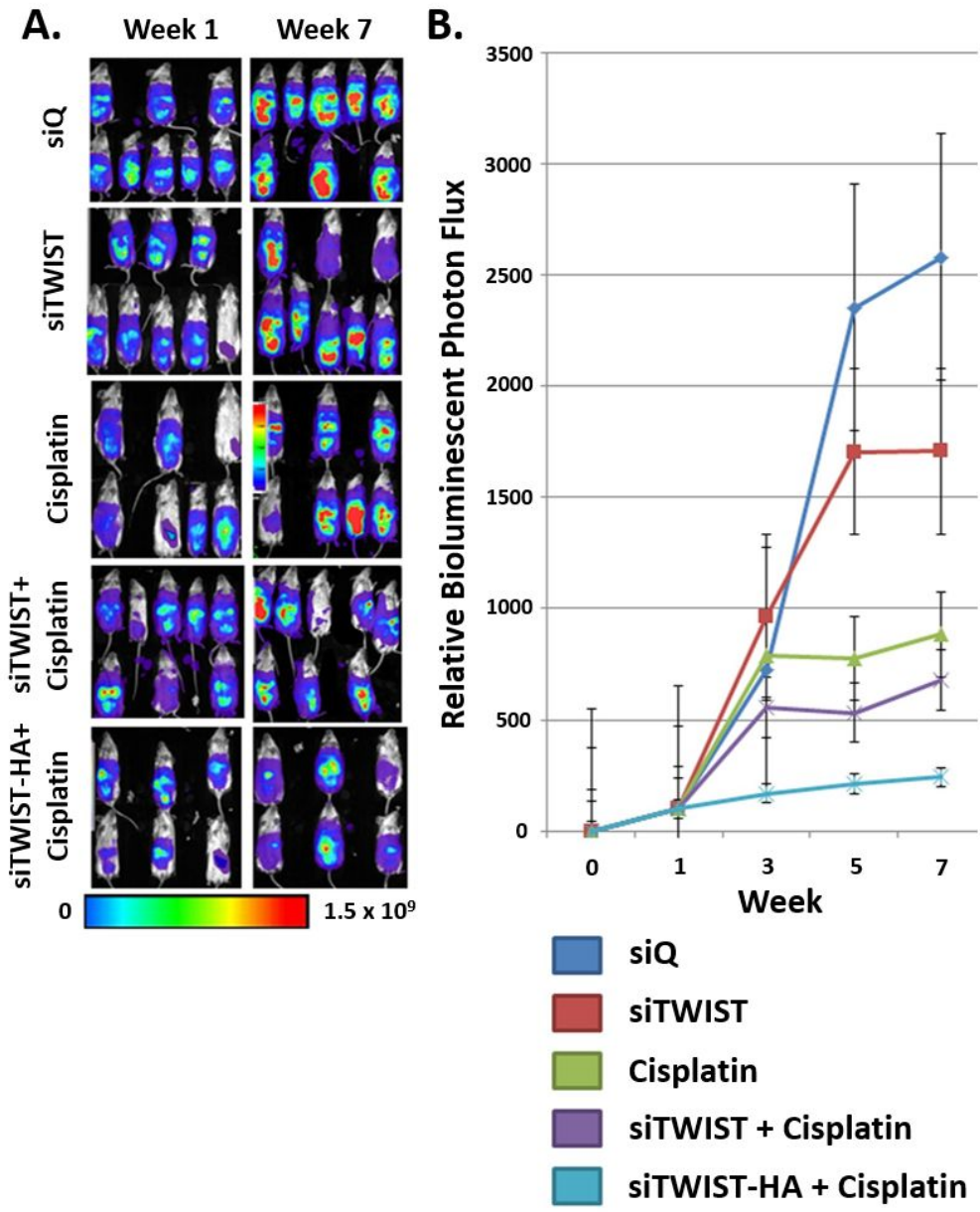

FIGURE 2. (A) Bioluminescence imaging of Ovcar8-IP tumors. Tumors treated with cisplatin emit noticeably weaker signal than siTWIST or siQ only control mice, while those treated with siTWIST-MSNs plus cisplatin exhibit a further loss of signal. siTWIST-MSN-HAs plus cisplatin exhibit a greatest loss of signal. (B) Quantification of bioluminescence depicted in A. Units for luminescence are photons/sec/cm^2/steradian. Adapted with permission from ref. 35. Copyright 2018 Elsevier.

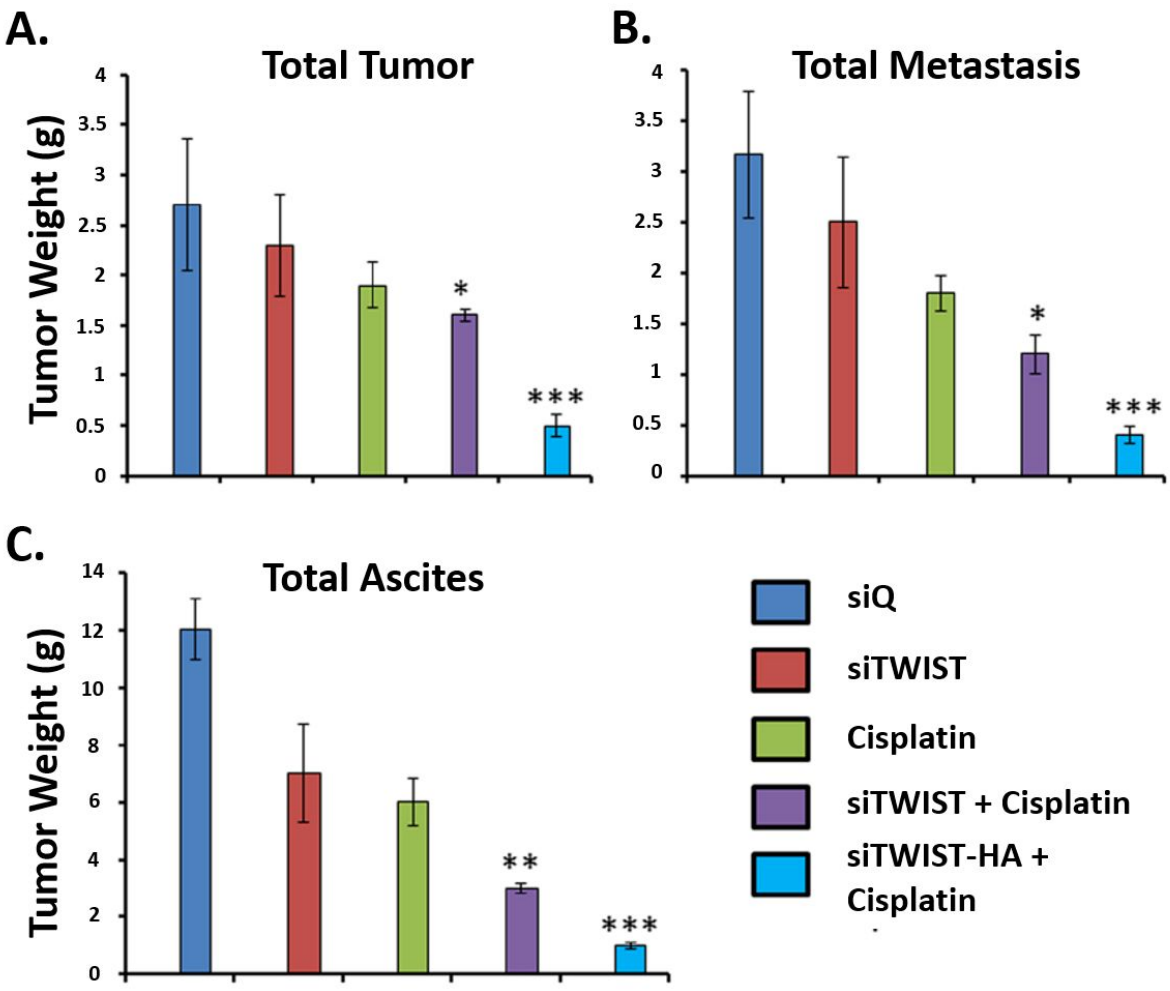

FIGURE 3. Quantification of the weight loss of (A) tumor, (B) metastasis, and (C) ascites of mice treated as described in Figure 2. The combination of HA targeted MSNs carrying siRNA and cisplatin was the most efficacious. Adapted with permission from ref. 35. Copyright 2018 Elsevier.

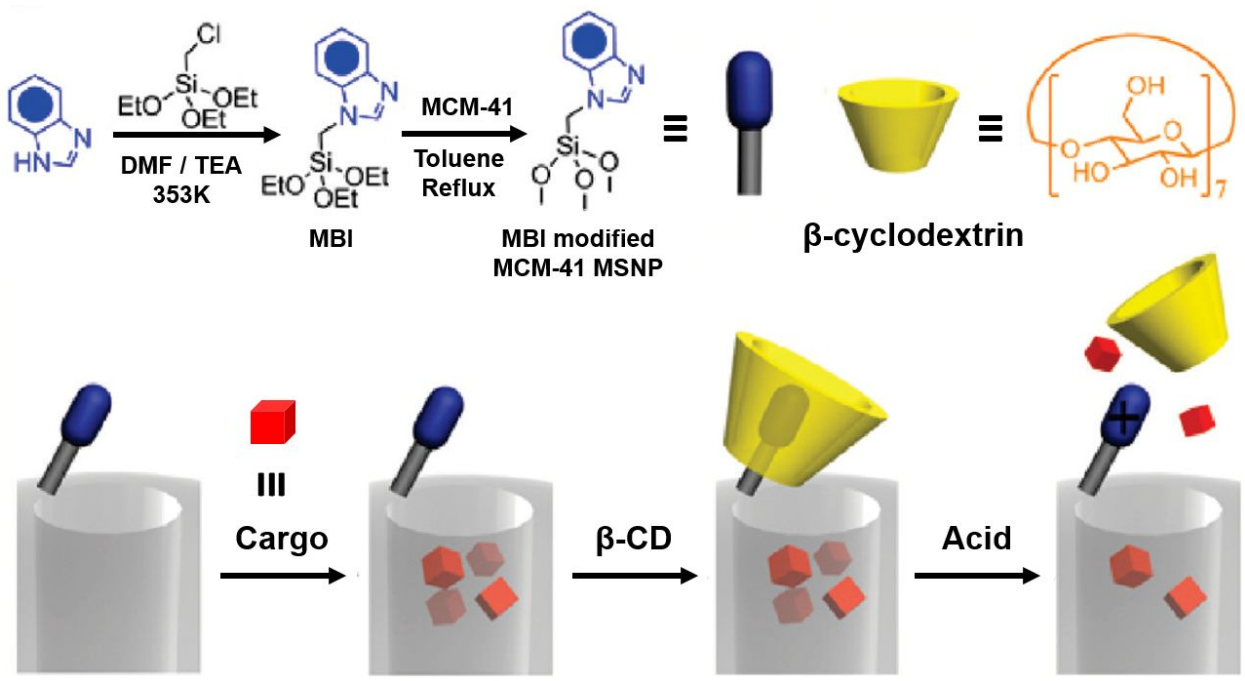

FIGURE 4. Schematic illustration of the pH-responsive benzimidazole nanovalve. Adapted with permission from ref. 37. Copyright (2018) American Chemical Society.

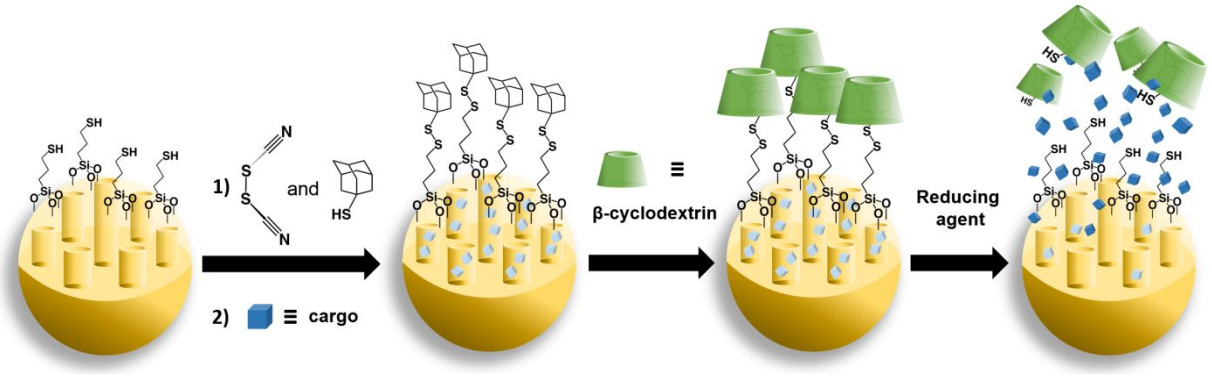

FIGURE 5. Schematic illustration of the redox-responsive disulfide nanovalve.

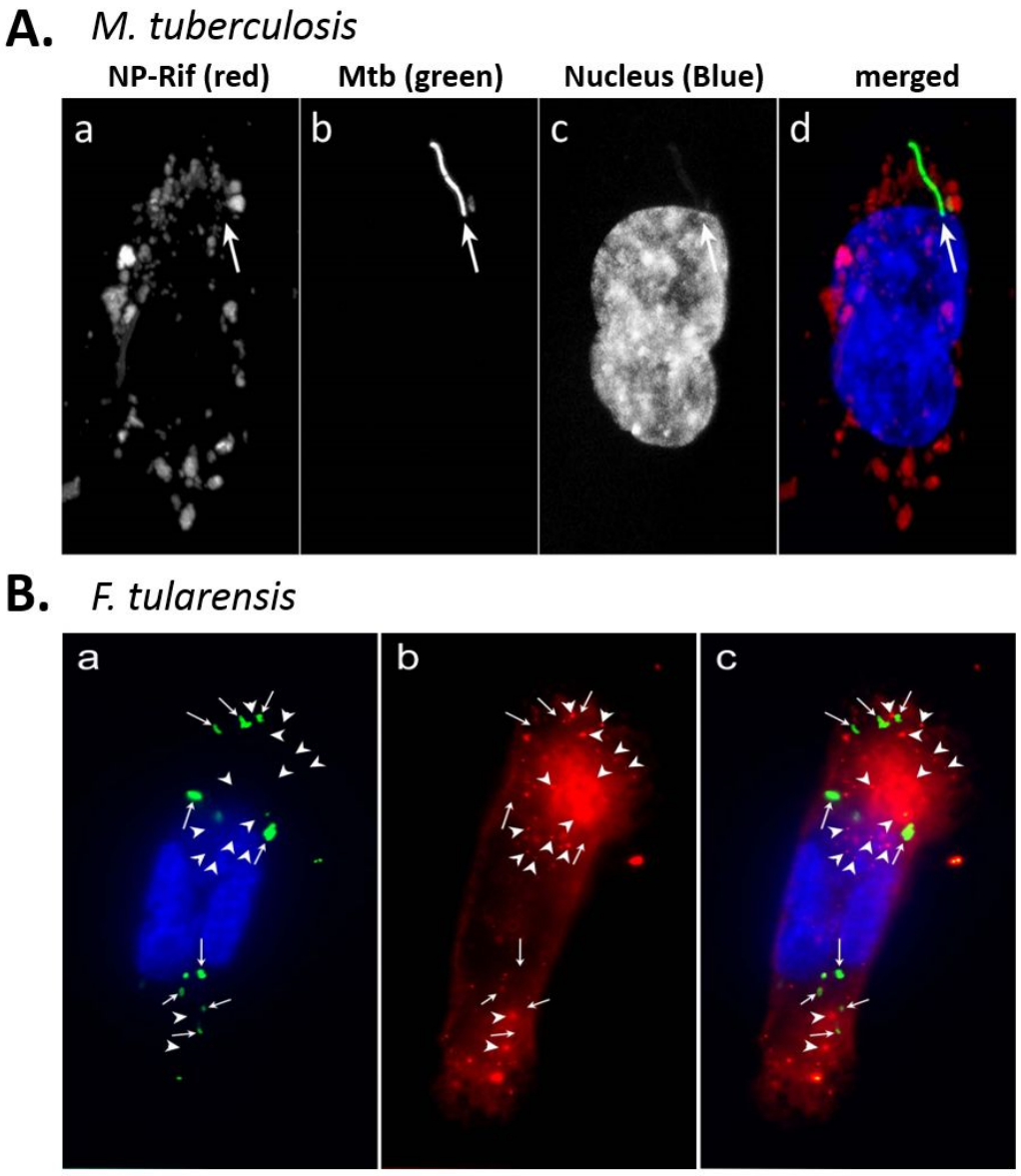

FIGURE 6. MSNs are avidly ingested by human macrophages infected with *Mycobacterium tuberculosis* (A) and *Francisella tularensis* (B). (A) Human THP-1 macrophages were infected with GFP-expressing Mtb, incubated with red fluorescent MSNs loaded with rifampin (NP-RIF), fixed, stained with nuclear stain DAPI, and imaged by confocal microscopy. Large numbers of NP-RIF (a) and an Mtb bacillus (b, arrow) are observed in the macrophage, whose nucleus is stained blue (c); the merged image is shown in panel d. Adapted with permission from ref. 41. Copyright 2012 American Society for Microbiology. (B) Human THP-1 macrophages were infected with GFP-expressing Ft, incubated with RITC-labelled MSN-MBI, fixed, stained with DAPI, and imaged by confocal microscopy. Green Ft (a, c, arrows), red MSNs (b, c, arrowheads) and DAPI-stained nucleus (a, c, blue) are seen in individual images (a, b) and merged image (c). Adapted with permission from ref. 42. Copyright 2015 American Chemical Society.

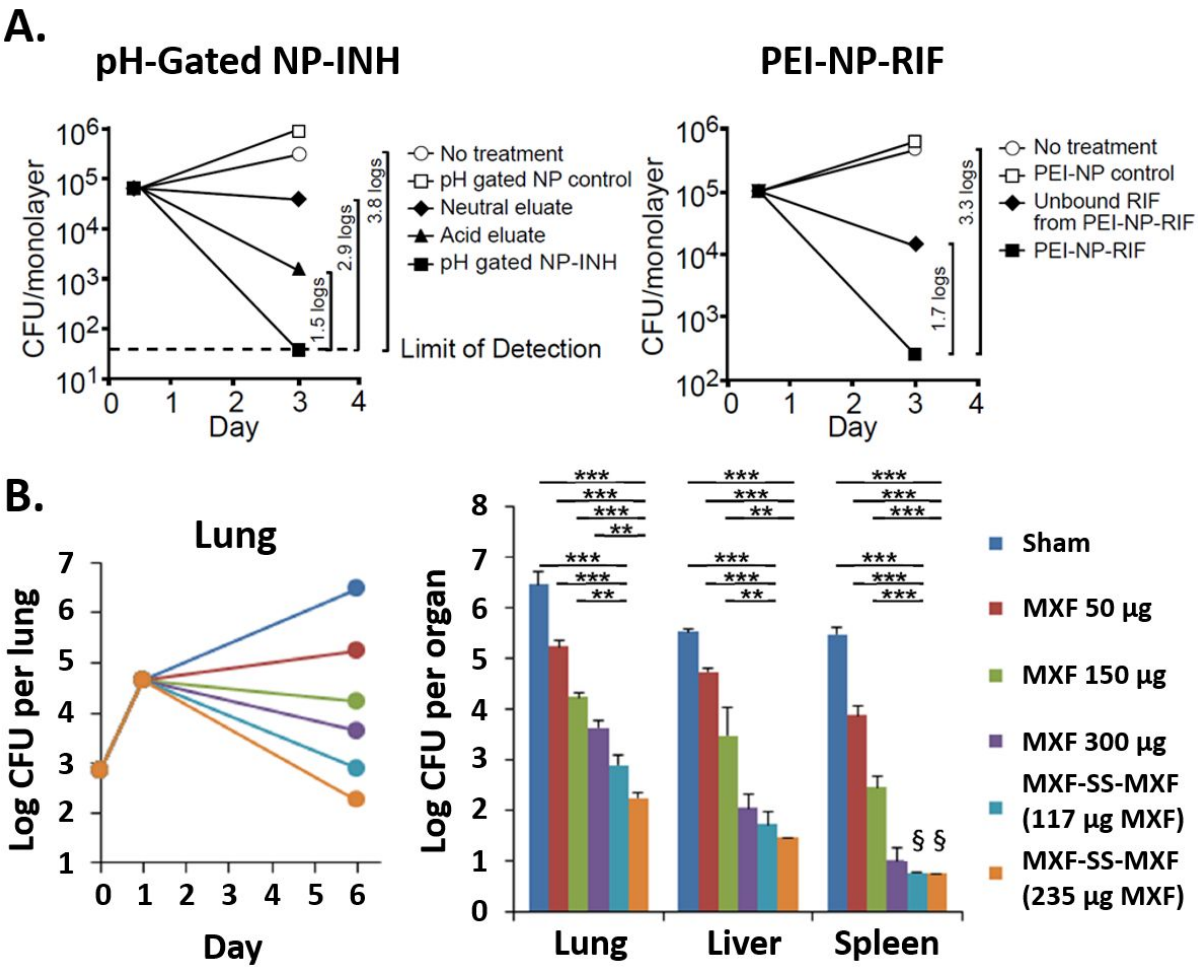

FIGURE 7. Antibiotic-loaded MSNs rapidly kill *M. tuberculosis in vitro* (A) and *F. tularensis in vivo* (B). (A) MSNs loaded with Isoniazid (INH) or Rifampin (RIF) kill Mtb to a greater extent than an equivalent amount of free drug. Compared with no treatment, the INH- and RIF-loaded MSNs reduced the colony-forming units (CFU) by 3.8 and 3.3 log CFU, respectively, and compared with an equivalent amount of free drug, they reduced CFU by an additional 1.5 and 1.7 log CFU, respectively. Adapted with permission from ref. 41. Copyright 2012 American Society for Microbiology. (B) MXF-loaded MSNs rapidly kill Ft *in vivo* in a mouse model of lethal pneumonic tularemia and are much more efficacious in reducing the lung burden of Ft than equivalent amounts of free MXF (Efficacy ratios 3-5:1).[43] The CFUs in lung, liver and spleen were determined on day 6. Adapted with permission from ref. 43. Copyright 2016 Wiley-VCH.

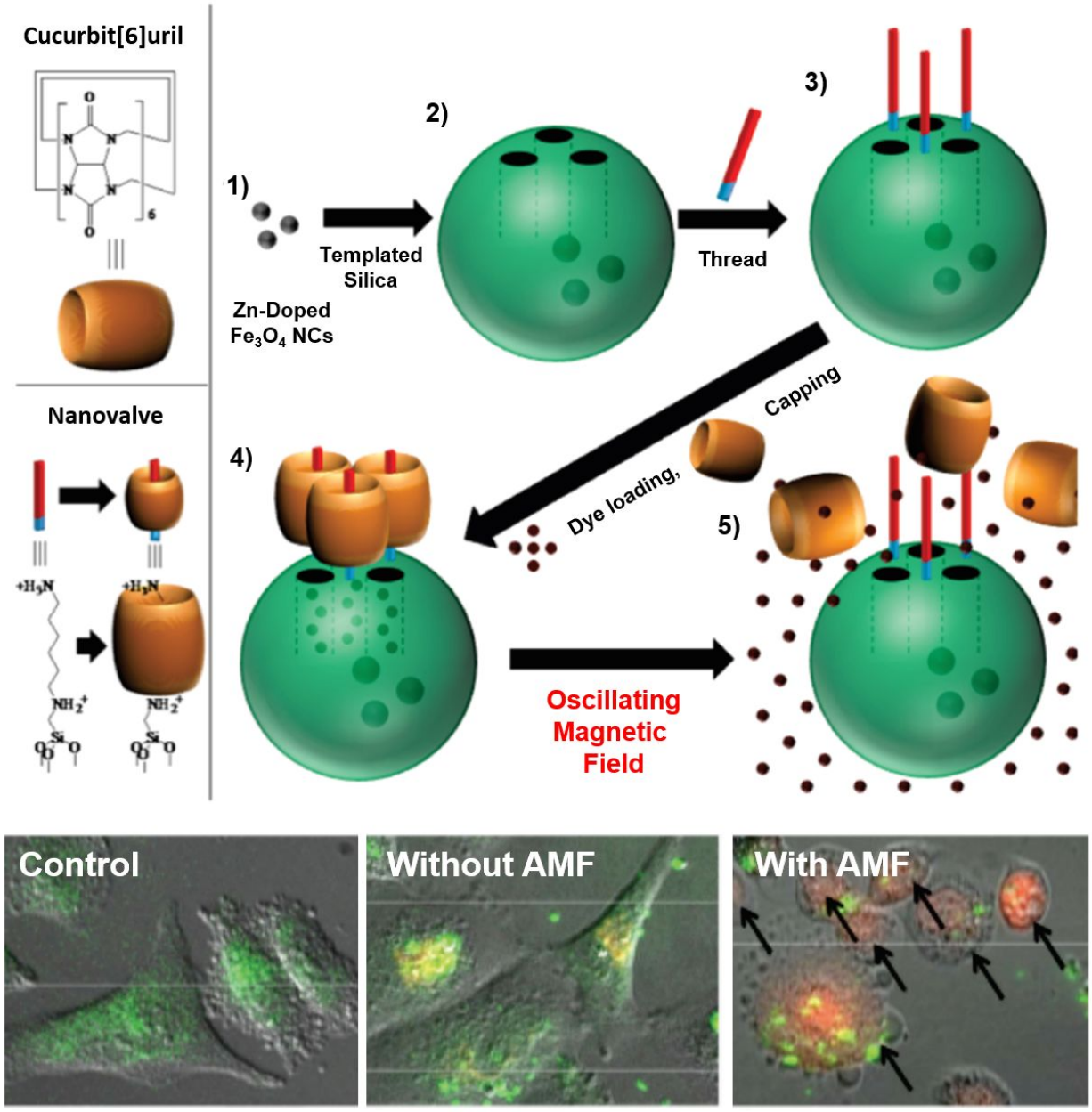

FIGURE 8. Schematic illustration of the construction and operation of the thermo-responsive cucurbit[6]uril nanovalve. Fluorescence microscope images show breast cancer cells were killed by the released DOX after the exposure to an AMF. Adapted with permission from ref. 61. Copyright 2010 American Chemical Society.

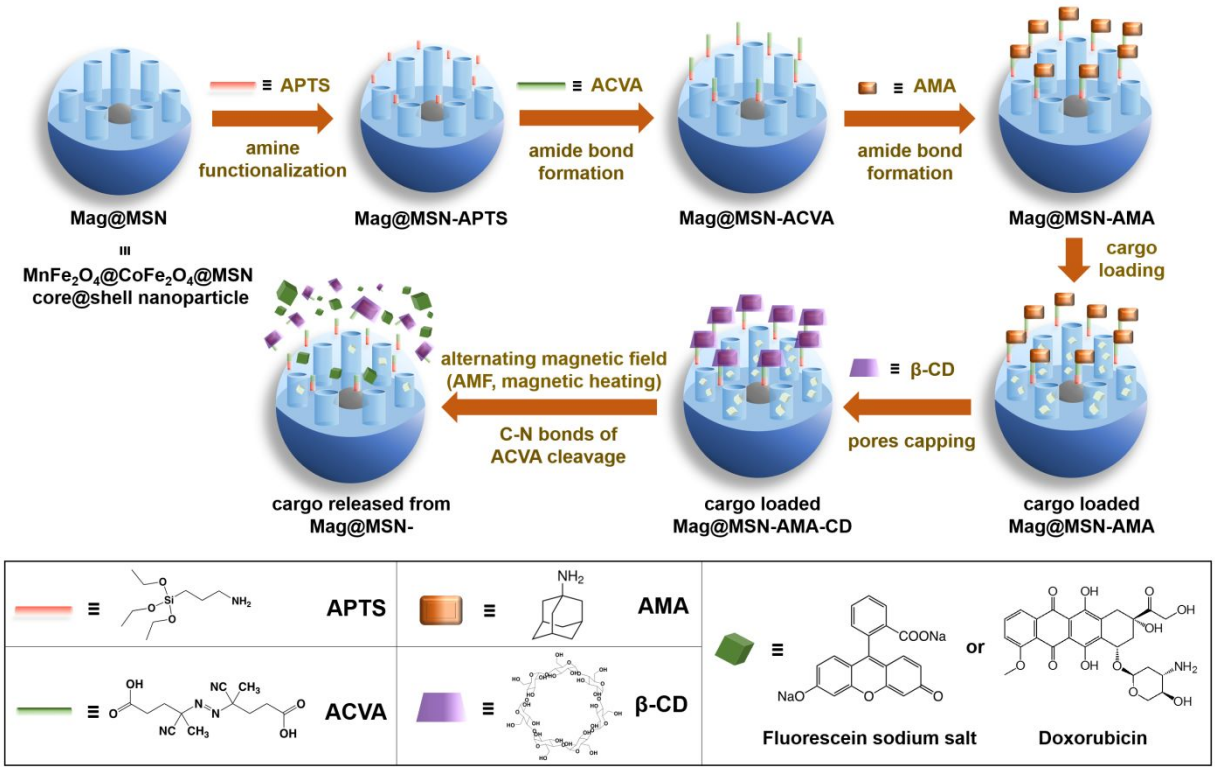

FIGURE 9. Schematic illustration of the synthesis and operation of the thermo-sensitive azo cap. Adapted with permission from ref. 62. Copyright 2019 American Chemical Society.

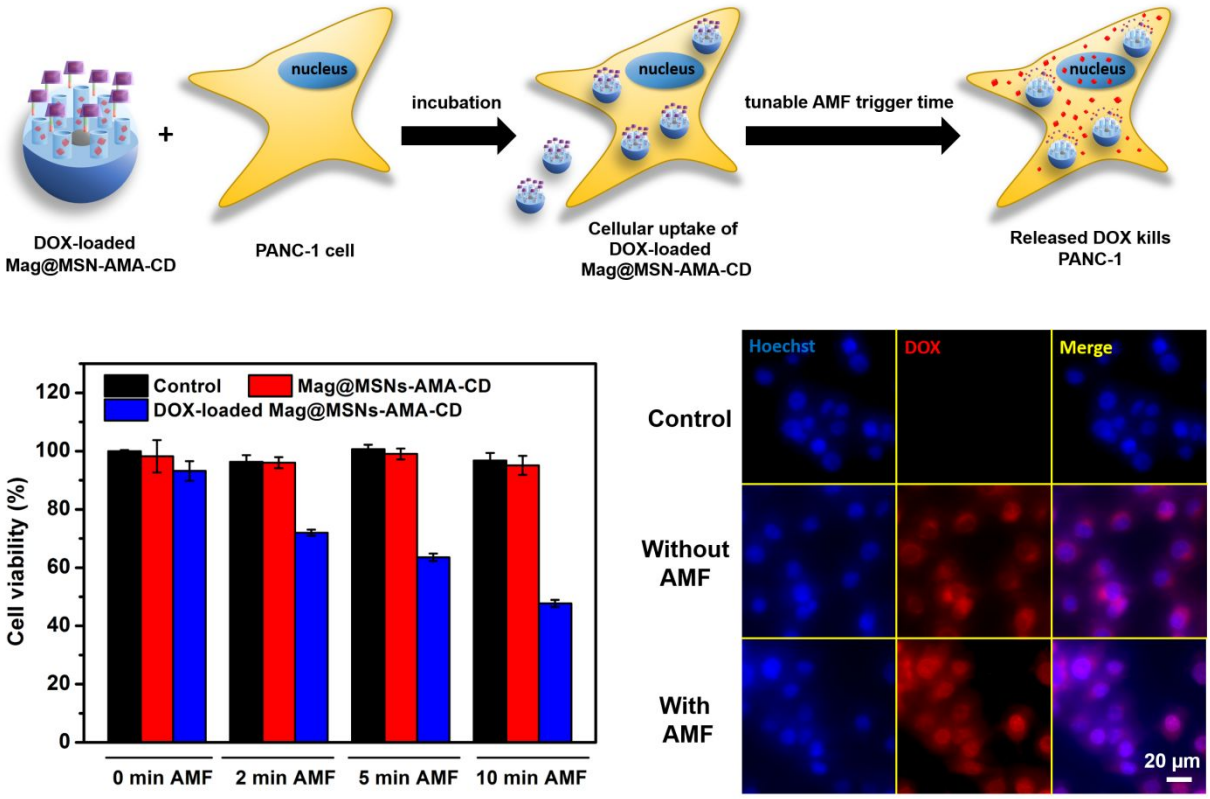

FIGURE 10. Effects of AMF stimulated DOX release on PANC-1 cells. *In vitro* cellular killing and fluorescence microscope images of DOX-loaded nanoparticles after AMF exposure are shown left and right, respectively. Adapted with permission from ref. 62. Copyright 2019 American Chemical Society.

ASSOCIATED CONTENT

The authors declare no competing financial interest.

AUTHOR INFORMATION

Corresponding Author

*zink@chem.ucla.edu

Author Contributions

The manuscript was written with contributions by all authors.

ORCID

Wei Chen: 0000-0002-2909-3023

Jeffrey I. Zink: 0000-0002-9792-4976

ACKNOWLEDGMENT

The authors gratefully acknowledge financial support through the years by the National Science Foundation, the National Institutes of Health, and the Defense Threat Reduction Agency. Manuscript writing was supported in part by the Zink Research and Student Support Fund.

Biographical Information

Wei Chen was born in Nantou, Taiwan. He received his B.S. and M.S. degrees in chemistry from National Taiwan University, where he did research under Professor Chung-Yuan Mou. He is currently a PhD student at UCLA Chemistry & Biochemistry Department under the supervision of Professor Jeffrey I. Zink. His research focuses on mesoporous silica-based imaging and drug delivery systems.

Carlotta A. Glackin is an Associate Professor in the Department of Developmental and Stem Cell Biology and an associate member of the Women's Cancers and Molecular Cellular Biology of Cancer (MCBC) Programs at the City of Hope Comprehensive Cancer Center (COHCCC). She received her PhD from University of Southern California, and her Postdoctoral training at the California Institute of Technology. Her research group is focuses on understanding the mechanisms of *TWIST*-mediated epithelial to mesenchymal transition (EMT) and developing therapeutic agents to inhibit *TWIST* in cancer.

Marcus A. Horwitz is Distinguished Professor of Medicine and Microbiology, Immunology & Molecular Genetics and formerly Chief of the Division of Infectious Diseases at UCLA. He received his M.D. degree from Columbia University College of Physicians & Surgeons and he trained and served on the faculty at The Rockefeller University. His research has focused on intracellular parasitism, especially the immunobiology of the etiologic agents of Legionnaires' disease, leprosy, tuberculosis, and tularemia and the development of vaccines, drugs, and nanotherapeutics against these pathogens.

Jeffrey I. Zink is a Distinguished Professor of Chemistry and Biochemistry and Co-director of the Cancer Molecular Imaging, Nanotechnology and Theranostics Program at the Jonsson Comprehensive Cancer Center at UCLA. He received his PhD degree from the University of

Illinois. He is the author of more than 500 publications and his current research interests include multifunctional nanomaterials and theranostic applications.

REFERENCES

(1) Brinker, C. J.; Scherer. G. W. *Sol-Gel Science: The Physics and Chemistry of Sol-Gel Processing*; Academic Press: Cambridge, 1990.

(2) Ellerby, L. M.; Nishida, C. R.; Nishida, F.; Yamanaka, S. A.; Dunn, B.; Valentine, J. S.; Zink, J. I. Encapsulation of Proteins in Transparent Porous Silicate Glasses Prepared by the Sol-Gel Method. *Science,* **1992**, *255*, 1113–1115.

(3) Chung, K. E.; Valentine, J. S.; Zink, J. I.; Lan, E. H.; Davidson, M. S.; Dunn, B. S. Measurement of Dissolved Oxygen in Water Using Glass-Encapsulated Myoglobin. *Anal. Chem.* **1995**, *67*, 1505–1509.

(4) Dunn, B.; Miller, J. M.; Dave, B. C.; Valentine, J. S.; Zink, J. I. Strategies for Encapsulating Biomolecules in Sol-Gel Matrices. *Acta Mater.* **1998**, *46*, 737–741.

(5) Miller, J. M.; Dunn, B.; Valentine, J. S.; Zink, J. I. Synthesis Conditions for Encapsulating Cytochrome c and Catalase in SiO_2 Sol-Gel Materials. *J. Non. Cryst. Solids* **1996**, *202*, 279–289.

(6) Kresge, C. T.; Leonowicz, M. E.; Roth, W. J.; Vartuli, J. C.; Beck, J. S. Ordered Mesoporous Molecular Sieves Synthesized by a Liquid-Crystal Template Mechanism. *Nature* **1992**, *359*, 710–712.

(7) Chiola, V.; Ritsko, J. E.; Vanderpool, C. D. Process for Producing Low-Bulk Density Silica, **1971** US Patent App 3556725A.

(8) Nishida, F.; McKiernan, J. M.; Dunn, B.; Zink, J. I.; Brinker, C. J.; Hurd, A. J. In Situ Fluorescence Probing of the Chemical Changes during Sol–Gel Thin Film Formation. *J. Am. Ceram. Soc.* **1995**, *78*, 1640–1648.

(9) Dave, B. C.; Soyez, H.; Miller, J. M.; Dunn, B.; Valentine, J. S.; Zink, J. I. Synthesis of Protein-Doped Sol-Gel SiO_2 Thin Films: Evidence for Rotational Mobility of Encapsulated Cytochrome C. *Chem. Mater.* **1995**, *7*, 1431–1434.

(10) Huang, M. H.; Dunn, B. S.; Soyez, H.; Zink, J. I. In Situ Probing by Fluorescence Spectroscopy of the Formation of Continuous Highly-Ordered Lamellar-Phase Mesostructured Thin Films. *Langmuir* **1998**, *14*, 7331–7333.

(11) Huang, M. H.; Dunn, B. S.; Zink, J. I. In Situ Luminescence Probing of the Chemical and Structural Changes during Formation of Dip-Coated Lamellar Phase Sodium Dodecyl Sulfate Sol-Gel Thin Films. *J. Am. Chem. Soc.* **2000**, *122*, 3739–3745.

(12) Grün, M.; Lauer, I.; Unger, K. K. The Synthesis of Micrometer- and Submicrometer-Size Spheres of Ordered Mesoporous Oxide MCM-41. *Adv. Mater.* **1997**, *9*, 254–257.

(13) Li, Z.; Barnes, J. C.; Bosoy, A.; Stoddart, J. F.; Zink, J. I. Mesoporous Silica Nanoparticles in Biomedical Applications. *Chem. Soc. Rev.* **2012**, *41*, 2590–2605.

(14) Ambrogio, M. W.; Thomas, C. R.; Zhao, Y. L.; Zink, J. I.; Stoddart, J. F. Mechanized Silica Nanoparticles: A New Frontier in Theranostic Nanomedicine. *Acc. Chem. Res.* **2011**, *44*, 903–913.

(15) Cotí, K. K.; Belowich, M. E.; Liong, M.; Ambrogio, M. W.; Lau, Y. A.; Khatib, H. A.; Zink, J. I.; Khashab, N. M.; Stoddart, J. F. Mechanised Nanoparticles for Drug Delivery. *Nanoscale* **2009**, 1, 16–39.

(16) Tarn, D.; Ashley, C. E.; Xue, M.; Carnes, E. C.; Zink, J. I.; Brinker, C. J. Mesoporous Silica Nanoparticle Nanocarriers: Biofunctionality and Biocompatibility. *Acc. Chem. Res.* **2013**, *46*, 792–801.

(17) Chen, W.; Tsai, P. H.; Hung, Y.; Chiou, S. H.; Mou, C. Y. Nonviral Cell Labeling and Differentiation Agent for Induced Pluripotent Stem Cells Based on Mesoporous Silica Nanoparticles. *ACS Nano*, **2013**, *7*, 8423–8440.

(18) Klichko, Y.; Liong, M.; Choi, E.; Angelos, S.; Nel, A. E.; Stoddart, J. F.; Tamanoi, F.; Zink, J. I. Mesostructured Silica for Optical Functionality, Nanomachines, and Drug Delivery. *J. Am. Ceram. Soc.* **2009**, *92*, S2-S10.

(19) Liong, M.; Lu, J.; Kovochich, M.; Xia, T.; Ruehm, S. G.; Nel, A. E.; Tamanoi, F.; Zink, J. I. Multifunctional Inorganic Nanoparticles for Imaging, Targeting, and Drug Delivery. *ACS Nano* **2008**, *2*, 889–896.
(20) Kumar, N.; Chen, W.; Cheng, C. A.; Deng, T.; Wang, R.; Zink, J. I. Stimuli-Responsive Nanomachines and Caps for Drug Delivery. *The Enzymes*, **2018**, *43*, 31–65.
(21) Lu, J.; Liong, M.; Zink, J. I.; Tamanoi, F. Mesoporous Silica Nanoparticles as a Delivery System for Hydrophobic Anticancer Drugs. *Small* **2007**, *3*, 1341–1346.
(22) Croissant, J. G.; Fatieiev, Y.; Julfakyan, K.; Lu, J.; Emwas, A. H.; Anjum, D. H.; Omar, H.; Tamanoi, F.; Zink, J. I.; Khashab, N. M. Biodegradable Oxamide-Phenylene-Based Mesoporous Organosilica Nanoparticles with Unprecedented Drug Payloads for Delivery in Cells. *Chem. Eur. J.* **2016**, *22*, 14806-14811.
(23) Chen, W.; Cheng, C. A.; Lee, B. Y.; Clemens, D. L.; Huang, W. Y.; Horwitz, M. A.; Zink, J. I. Facile Strategy Enabling Both High Loading and High Release Amounts of the Water-Insoluble Drug Clofazimine Using Mesoporous Silica Nanoparticles. *ACS Appl. Mater. Interfaces* **2018**, *10*, 31870–31881.
(24) Ferris, D. P.; Lu, J.; Gothard, C.; Yanes, R.; Thomas, C. R.; Olsen, J. C.; Stoddart, J. F.; Tamanoi, F.; Zink, J. I. Synthesis of Biomolecule-Modified Mesoporous Silica Nanoparticles for Targeted Hydrophobic Drug Delivery to Cancer Cells. *Small* **2011**, *7*, 1816–1826.
(25) Xia, T.; Kovochich, M.; Liong, M.; Meng, H.; Kabehie, S.; George, S.; Zink, J. I.; Nel, A. E. Polyethyleneimine Coating Enhances the Cellular Uptake of Mesoporous Silica Nanoparticles and Allows Safe Delivery of siRNA and DNA Constructs. *ACS Nano* **2009**, *3*, 3273–3286.
(26) Meng, H.; Xue, M.; Xia, T.; Ji, Z.; Tarn, D. Y.; Zink, J. I.; Nel, A. E. Use of Size and a Copolymer Design Feature to Improve the Biodistribution and the Enhanced Permeability and Retention Effect of Doxorubicin-Loaded Mesoporous Silica Nanoparticles in a Murine Xenograft Tumor Model. *ACS Nano* **2011**, *5*, 4131–4144.
(27) Sontheimer, E. J. Assembly and Function of RNA Silencing Complexes. *Nat. Rev. Mol. Cell Biol.* **2005**, *6*, 127–138.
(28) Fire, A.; Xu, S.; Montgomery, M. K.; Kostas, S. A.; Driver, S. E.; Mello, C. C. Potent and Specific Genetic Interference by Double-Stranded RNA in Caenorhabditis Elegans. *Nature* **1998**, 391, 806–811.
(29) Elbashir, S. M.; Harborth, J.; Lendeckel, W.; Yalcin, A.; Weber, K.; Tuschl, T. Duplexes of 21-Nucleotide RNAs Mediate RNA Interference in Cultured Mammalian Cells. *Nature* **2001**, *411*, 494–498.
(30) Tijsterman, M.; Plasterk, R. H. A. Dicers at RISC: The Mechanism of RNAi. *Cell*, **2004**, *117*, 1–3.
(31) Liu, J.; Carmell, M. A.; Rivas, F. V.; Marsden, C. G.; Thomson, J. M.; Song, J. J.; Hammond, S. M.; Joshua-Tor, L.; Hannon, G. J. Argonaute2 Is the Catalytic Engine of Mammalian RNAi. *Science* **2004**, 305, 1437–1441.
(32) Meng, H.; Mai, W. X.; Zhang, H.; Xue, M.; Xia, T.; Lin, S.; Wang, X.; Zhao, Y.; Ji, Z.; Zink, J. I.; Nel, A. E. Codelivery of an Optimal Drug/siRNA Combination Using Mesoporous Silica Nanoparticles to Overcome Drug Resistance in Breast Cancer *in Vitro* and *in Vivo*. *ACS Nano* **2013**, 7, 994–1005.
(33) Finlay, J.; Roberts, C. M.; Dong, J.; Zink, J. I.; Tamanoi, F.; Glackin, C. A. Mesoporous Silica Nanoparticle Delivery of Chemically Modified siRNA against TWIST1 Leads to Reduced Tumor Burden. *Nanomedicine* **2015**, *11*, 1657–1666.
(34) Roberts, C. M.; Shahin, S. A.; Wen, W.; Finlay, J. B.; Dong, J.; Wang, R.; Dellinger, T. H.; Zink, J. I.; Tamanoi, F.; Glackin, C. A. Nanoparticle Delivery of siRNA against TWIST to Reduce Drug Resistance and Tumor Growth in Ovarian Cancer Models. *Nanomedicine* **2017**, *13*, 965–976.
(35) Shahin, S. A.; Wang, R.; Simargi, S. I.; Contreras, A.; Parra Echavarria, L.; Qu, L.; Wen, W.; Dellinger, T.; Unternaehrer, J.; Tamanoi, F.; Zink, J. I.; Glackin, C. A. Hyaluronic Acid Conjugated Nanoparticle Delivery of siRNA against TWIST Reduces Tumor Burden and Enhances Sensitivity to Cisplatin in Ovarian Cancer. *Nanomedicine* **2018**, *14*, 1381–1394.

(36) Ruehle, B.; Saint-Cricq, P.; Zink, J. I. Externally Controlled Nanomachines on Mesoporous Silica Nanoparticles for Biomedical Applications. *Chemphyschem* **2016**, *17*, 1769–1779.
(37) Meng, H.; Xue, M.; Xia, T.; Zhao, Y. L.; Tamanoi, F.; Stoddart, J. F.; Zink, J. I.; Nel, A. E. Autonomous *in Vitro* Anticancer Drug Release from Mesoporous Silica Nanoparticles by pH-Sensitive Nanovalves. *J. Am. Chem. Soc.* **2010**, *132*, 12690–12697.
(38) Ambrogio, M. W.; Pecorelli, T. A.; Patel, K.; Khashab, N. M.; Trabolsi, A.; Khatib, H. A.; Botros, Y. Y.; Zink, J. I.; Stoddart, J. F. Snap-Top Nanocarriers. *Org. Lett.* **2010**, 12, 3304–3307.
(39) Patel, K.; Angelos, S.; Dichtel, W. R.; Coskun, A.; Yang, Y. W.; Zink, J. I.; Stoddart, J. F. Enzyme-Responsive Snap-Top Covered Silica Nanocontainers. *J. Am. Chem. Soc.* **2008**, *130*, 2382–2383.
(40) Hwang, A. A.; Lee, B. Y.; Clemens, D. L.; Dillon, B. J.; Zink, J. I.; Horwitz, M. A. pH-Responsive Isoniazid-Loaded Nanoparticles Markedly Improve Tuberculosis Treatment in Mice. *Small* **2015**, *11*, 5066–5078.
(41) Clemens, D. L.; Lee, B. Y.; Xue, M.; Thomas, C. R.; Meng, H.; Ferris, D.; Nel, A. E.; Zink, J. I.; Horwitz, M. A. Targeted Intracellular Delivery of Antituberculosis Drugs to Mycobacterium Tuberculosis-Infected Macrophages via Functionalized Mesoporous Silica Nanoparticles. *Antimicrob. Agents Chemother.* **2012**, *56*, 2535–2545.
(42) Li, Z.; Clemens, D. L.; Lee, B. Y.; Dillon, B. J.; Horwitz, M. A.; Zink, J. I. Mesoporous Silica Nanoparticles with pH-Sensitive Nanovalves for Delivery of Moxifloxacin Provide Improved Treatment of Lethal Pneumonic Tularemia. *ACS Nano* **2015**, *9*, 10778–10789.
(43) Lee, B. Y.; Li, Z.; Clemens, D. L.; Dillon, B. J.; Hwang, A. A.; Zink, J. I.; Horwitz, M. A. Redox-Triggered Release of Moxifloxacin from Mesoporous Silica Nanoparticles Functionalized with Disulfide Snap-Tops Enhances Efficacy Against Pneumonic Tularemia in Mice. *Small* **2016**, *27*, 3690–3702.
(44) Guardado-Alvarez, T. M.; Russell, M. M.; Zink, J. I. Nanovalve Activation by Surface-Attached Photoacids. *Chem. Commun.* **2014**, *50*, 8388–8390.
(45) Saha, S.; Johansson, E.; Flood, A. H.; Tseng, H. R.; Zink, J. I.; Stoddart, J. F. A Photoactive Molecular Triad as a Nanoscale Power Supply for a Supramolecular Machine. *Chem. Eur. J.* **2005**, *11*, 6846–6858.
(46) Lu, J.; Choi, E.; Tamanoi, F.; Zink, J. I. Light-Activated Nanoimpeller-Controlled Drug Release in Cancer Cells. *Small* **2008**, *4*, 421–426.
(47) Angelos, S.; Choi, E.; Vögtle, F.; De Cola, L.; Zink, J. I. Photo-Driven Expulsion of Molecules from Mesostructured Silica Nanoparticles. *J. Phys. Chem. C* **2007**, *111*, 6589–6592.
(48) Lau, Y. A.; Henderson, B. L.; Lu, J.; Ferris, D. P.; Tamanoi, F.; Zink, J. I. Continuous Spectroscopic Measurements of Photo-Stimulated Release of Molecules by Nanomachines in a Single Living Cell. *Nanoscale* **2012**, *4*, 3482–3489.
(49) Ferris, D. P.; Zhao, Y. L.; Khashab, N. M.; Khatib, H. A.; Stoddart, J. F.; Zink, J. I. Light-Operated Mechanized Nanoparticles. *J. Am. Chem. Soc.* **2009**, *131*, 1686–1688.
(50) Tarn, D.; Ferris, D. P.; Barnes, J. C.; Ambrogio, M. W.; Stoddart, J. F.; Zink, J. I. A Reversible Light-Operated Nanovalve on Mesoporous Silica Nanoparticles. *Nanoscale* **2014**, *6*, 3335–3343.
(51) Guardado-Alvarez, T. M.; Sudha Devi, L.; Russell, M. M.; Schwartz, B. J.; Zink, J. I. Activation of Snap-Top Capped Mesoporous Silica Nanocontainers Using Two near-Infrared Photons. *J. Am. Chem. Soc.* **2013**, *135*, 14000–14003.
(52) Croissant, J.; Zink, J. I. Nanovalve-Controlled Cargo Release Activated by Plasmonic Heating. *J. Am. Chem. Soc.* **2012**, *134*, 7628–7631.
(53) Guardado-Alvarez, T. M.; Devi, L. S.; Vabre, J. M.; Pecorelli, T. A.; Schwartz, B. J.; Durand, J. O.; Mongin, O.; Blanchard-Desce, M.; Zink, J. I. Photo-Redox Activated Drug Delivery Systems Operating under Two Photon Excitation in the near-IR. *Nanoscale* **2014**, *6*, 4652–4658.
(54) Croissant, J.; Chaix, A.; Mongin, O.; Wang, M.; Clément, S.; Raehm, L.; Durand, J. O.; Hugues, V.; Blanchard-Desce, M.; Maynadier, M.; Gallud, A.; Gary-Bobo, M.; Garcia, M.; Lu, J.;

Tamanoi, F.; Ferris, D. P.; Tarn, D.; Zink J. I. Two-Photon-Triggered Drug Delivery via Fluorescent Nanovalves. *Small* **2014**, *10*, 1752–1755.

(55) Jang, J. T.; Nah, H.; Lee, J. H.; Moon, S. H.; Kim, M. G.; Cheon, J. Critical Enhancements of MRI Contrast and Hyperthermic Effects by Dopant-Controlled Magnetic Nanoparticles. *Angew. Chem. Int. Ed.* **2009**, *48*, 1234–1238.

(56) Lee, J. H.; Jang, J. T.; Choi, J. S.; Moon, S. H.; Noh, S. H.; Kim, J. W.; Kim, J. G.; Kim, I. S.; Park, K. I.; Cheon, J. Exchange-Coupled Magnetic Nanoparticles for Efficient Heat Induction. *Nat. Nanotechnol.* **2011**, *6*, 418–422.

(57) Noh, S. hyun; Moon, S. H.; Shin, T. H.; Lim, Y.; Cheon, J. Recent Advances of Magneto-Thermal Capabilities of Nanoparticles: From Design Principles to Biomedical Applications. *Nano Today*, **2017**, *13*, 61–76.

(58) Dong, J.; Zink, J. I. Taking the Temperature of the Interiors of Magnetically Heated Nanoparticles. *ACS Nano* **2014**, *8*, 5199–5207.

(59) Rühle, B.; Datz, S.; Argyo, C.; Bein, T.; Zink, J. I. A Molecular Nanocap Activated by Superparamagnetic Heating for Externally Stimulated Cargo Release. *Chem. Commun.* **2016**, *52*, 1843–1846.

(60) Saint-Cricq, P.; Deshayes, S.; Zink, J. I.; Kasko, A. M. Magnetic Field Activated Drug Delivery Using Thermodegradable Azo-Functionalised PEG-Coated Core–Shell Mesoporous Silica Nanoparticles. *Nanoscale* **2015**, *7*, 13168–13172.

(61) Thomas, C. R.; Ferris, D. P.; Lee, J. H.; Choi, E.; Cho, M. H.; Kim, E. S.; Stoddart, J. F.; Shin, J. S.; Cheon, J.; Zink, J. I. Noninvasive Remote-Controlled Release of Drug Molecules in Vitro Using Magnetic Actuation of Mechanized Nanoparticles. *J. Am. Chem. Soc.* **2010**, *132*, 10623–10625.

(62) Chen, W.; Cheng, C. A.; Zink, J. I. Spatial, Temporal, and Dose Control of Drug Delivery Using Noninvasive Magnetic Stimulation. *ACS Nano* **2019**, *13*, 1292–1308.

(63) Clemens, D. L.; Lee, B. Y.; Plamthottam, S.; Tullius, M. V.; Wang, R.; Yu, C J; Li, Z.; Dillon, B. J.; Zink, J. I.; Horwitz, M. A. Nanoparticle Formulation of Moxifloxacin and Intramuscular Route of Delivery Improve Antibiotic Pharmacokinetics and Treatment of Pneumonic Tularemia in a Mouse Model. *ACS Infect. Dis.* **2019**, 5, 281–291.

Table of Contents